

Deformation Characteristic of Thin Stainless Gasket Material

Shigeyuki Haruyama^{1,a}, Didik Nurhadiyanto^{2,b}, Kazuya Ushijima³,
Ken Kaminishi^{4,d}, Dai-Heng Chen⁵

¹Management of Technology, Yamaguchi University, 2-16-1 Tokiwadai, Ube-shi, Yamaguchi, Japan

²Doctoral student at Department of Mechanical Engineering, Yamaguchi University, Japan

Lecturer at Mechanical Education Engineering Department, Yogyakarta State University, Indonesia

³Department of Science and Engineering, Yamaguchi University, 2-16-1 Tokiwadai, Ube-shi,
Yamaguchi, Japan (Graduated 2013)

⁴Management of Technology, Yamaguchi University, 2-16-1 Tokiwadai, Ube-shi, Yamaguchi, Japan

⁵Tokyo University of Science, Faculty of Engineering, Kudankita 1-4-16, Chiyoda-ku, Tokyo,
102-0073, Japan

^aharuyama@yamaguchi-u.ac.jp, ^br502wc@yamaguchi-u.ac.jp, ^dkaminisi@yamaguchi-u.ac.jp

Keywords: Thin stainless, Gasket material, FEM, Deformation, Mode, Contact width

Abstract. Previous studies on corrugated metal gaskets have established that the contact width, contact stress, and surface roughness are important design parameters for optimizing gasket performance. However, the metal gaskets studied previously required a high axial force for the tightening process; in addition that metal gaskets tend to corrode easily. In this study, we examined the deformation mode of a thin stainless gasket using a finite element method (FEM) analysis. A final evaluation was made using a compression examination. The analysis based on the dimension of flat and convex portion. The load, deformation mode, and contact stress were obtained through a simulation. Based on the deformation of the flat and convex portions, the deformation modes were divided into three types. The deformation mode of the thin stainless gasket material has a higher probability of deformation in mode I when the aspect ratio of the length of the flat portion to the length of the convex portion, L/D , increases.

Introduction

As a replacement for gaskets containing asbestos material, many researchers have studied the use of metal gasket materials. Saeed *et al.* studied a new 25A-size corrugated metal gasket that was developed as an asbestos gasket substitute. The gasket had a metal spring effect and produced high local contact stress to create a sealing line with a flange. The results showed that the contact stress and contact width were important design parameters for optimizing the gasket performance [1]. Haruyama *et al.* [2] continued this research. The size limit of the contact width as a gasket design parameter was investigated. Comparing the results of FEM analysis of the relationship between the clamping load of the flange and the contact width with experimental results for the clamping load and leakage clarified the contact width with no leak for the new 25A-size metal gasket. Based on this result, the contact width can be used as a main parameter to optimize the gasket design. The leakage can be reduced by increasing the contact width. Chiron *et al.* [3] studied a validity method for contact width measurement using simulation analysis, and the result was compared with the result of an experiment using pressure-sensitive paper. Similar trends were seen in the simulation and experimental results. Nurhadiyanto *et al.* [4] used FEM to study a gasket design optimization method based on an elastic and plastic contact stress analysis that considered the forming effect. A helium leakage test showed that a gasket based on a plastic contact stress design was better than a gasket based on an elastic stress design. However, both types of gaskets could be used for seals because they did not leak in the helium leak test.

However, the 25-A size metal gasket requires a high axial force for the tightening process; moreover, a metal gasket has a tendency to corrode easily. To reduce the axial force and corrosion effect, we studied a thin stainless gasket material. Ushijima *et al.* [5] studied the deformation mode of a thin metal gasket based on an experiment and FEM. They compared the load and contact width-displacement curves obtained experimentally with those obtained analytically in a compression test, along with the deformed shape of a gasket. They classified the deformation modes into two types. In this paper, we present the results of a numerical analysis using FEM and an experimental analysis of a thin stainless gasket material. We investigate the deformation modes and classify them into three types. In addition, we investigate the displacement-contact stress and width curves.

Material and Method

Stainless steel was used as a gasket material because of its effectiveness at high temperature and its resistance to corrosion. Its material properties were determined through a tensile test carried out based on JIS2241 [6]. Based on the tensile test results, the nominal stress (σ) was 300.34 MPa, the modulus of the elasticity (E) was 48.67 GPa, the tangent modulus was 483.33 MPa, and Poisson's ratio was 0.3. Fig.1 shows the dimensions of the thin stainless gasket material used in this study, which were as follows: convex portion length $D = 20$ mm; height $h = 4.0$ mm; thickness $t = 0.3$ mm; distance from a central axis $r = 100$ mm. The length of the flat portion varied, with the following values: $L = 1.5$ mm, 2.0 mm, and 4.0 mm.

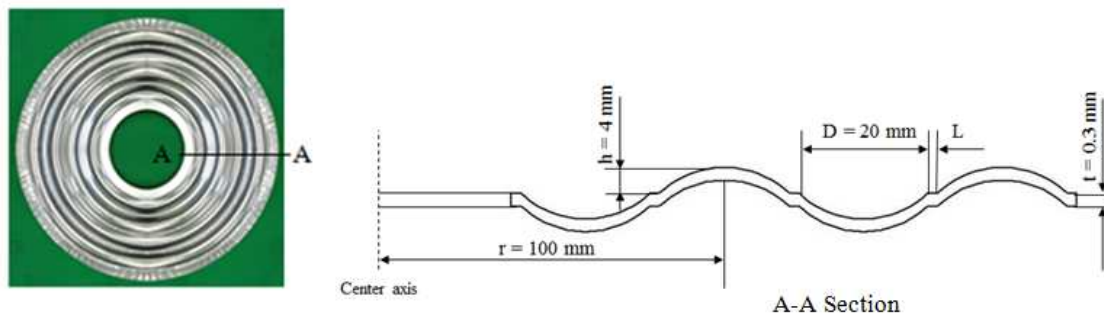


Fig. 1 Dimensions of thin stainless gasket material

Simulation Analysis. The deformation mode of the stainless gasket was investigated using an FEM analysis. The stages were modeled using the software MSC.marc. Using two-dimensional assumptions, an axis-symmetric shell element model was adopted for the tightening process simulation in the axial direction between the upper and lower flange. The FEM analysis for the tightening simulation is shown in Fig. 2. The gasket material model was compressed between the upper and lower rigid flanges using axial displacement to simulate the relationship between the load-displacement and contact width curves. Both the upper and lower flanges are assumed to be rigid bodies. The lower flange is assumed to have a fixed boundary condition. Further, the contact stress and contact width evaluation is performed only for the convex portion of the gasket, which is effective at reducing the leakage. The deformation mode evaluation is performed for the convex and flat portions.

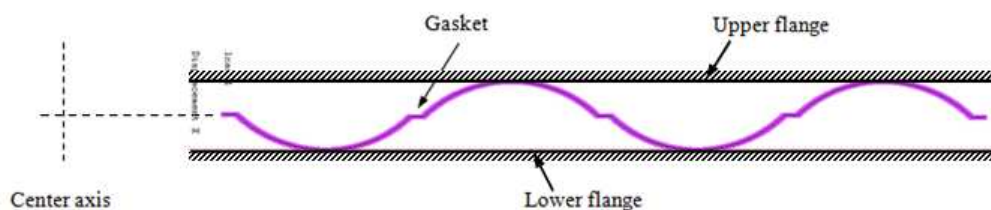


Fig. 2 FEM simulation model

Experimental Analysis. Fig. 3 shows a schematic diagram of the experimental compression device. We used a Tensilon large-sized testing machine (UTM-I-25000) for the compression process. The load and displacement were monitored using a laser displacement sensor (SUNX HL-C135C-BK10) and a sensor interface (Kyowa Electronic Instruments PCD300A) at a sampling speed of 20 Hz. The compression speed was set at 5 mm/min. The deformation mode of the stainless gasket was investigated using a compression test. The gasket was compressed between upper and lower rigid flanges using axial displacement. Both the upper and lower flanges were assumed to be rigid bodies. The lower flange has a fixed boundary condition. The upper flange moved in a downward direction and pressed the gasket. In order to verify the state of gasket deformation, we used silicone rubber. The silicone rubber was sandwiched and compressed between the gasket and upper flange, as shown in Fig. 4. We did not use lubricating oil to simulate a dry contact condition in the actual environment.

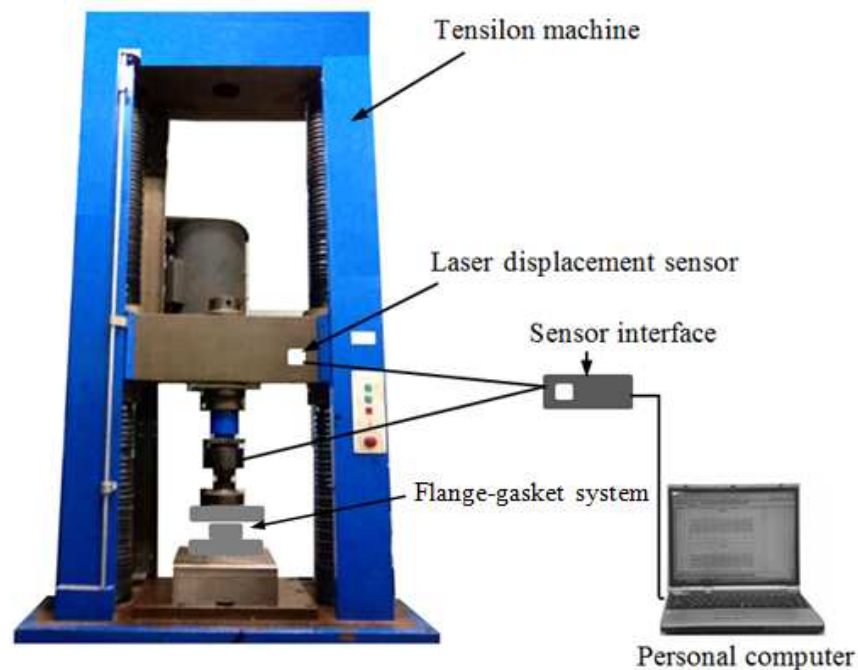


Fig. 3 Experimental apparatus

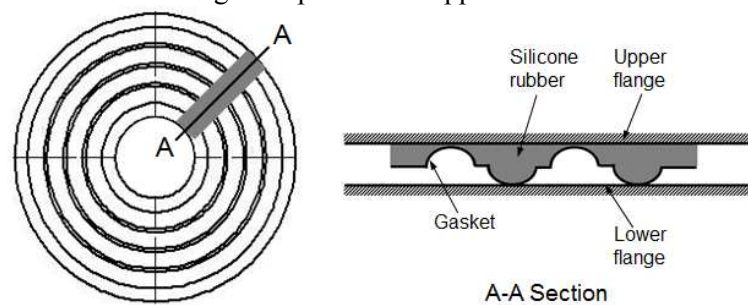


Fig. 4 Sandwiching silicone rubber

Results

The deformed shapes found in an FEM analysis and experimental analysis of a gasket having a flat portion $L = 4$ mm, 2 mm, and 1.5 mm are shown in Figs. 5, 6, and 7, respectively. Fig. 5 shows the deformed shape of a gasket with a flat portion of 4.0 mm. It could be determined that in this gasket, the deformation was concentrated in the flat portion, whereas most of convex portion 2 and 3 remained undeformed. We called this deformation mode I. This gasket did not provide a good seal. In the gaskets shown in Figs. 6 and 7, convex portion 3 was deformed and the contact width increased. We called this deformation mode II. We call the case where convex portion 2 was deformed and buckling protrusion occurred deformation mode III.

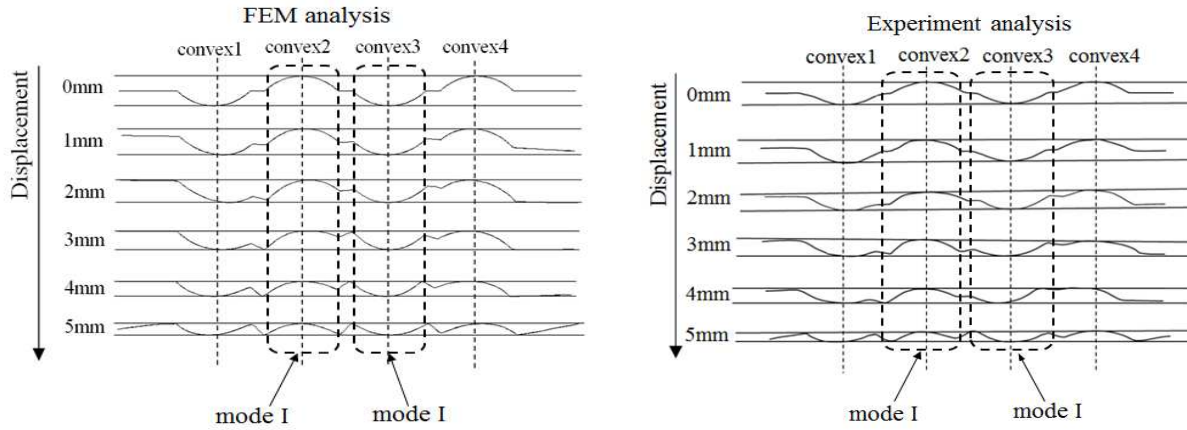


Fig. 5 Deformation mode for gasket having flat portion of 4.0 mm

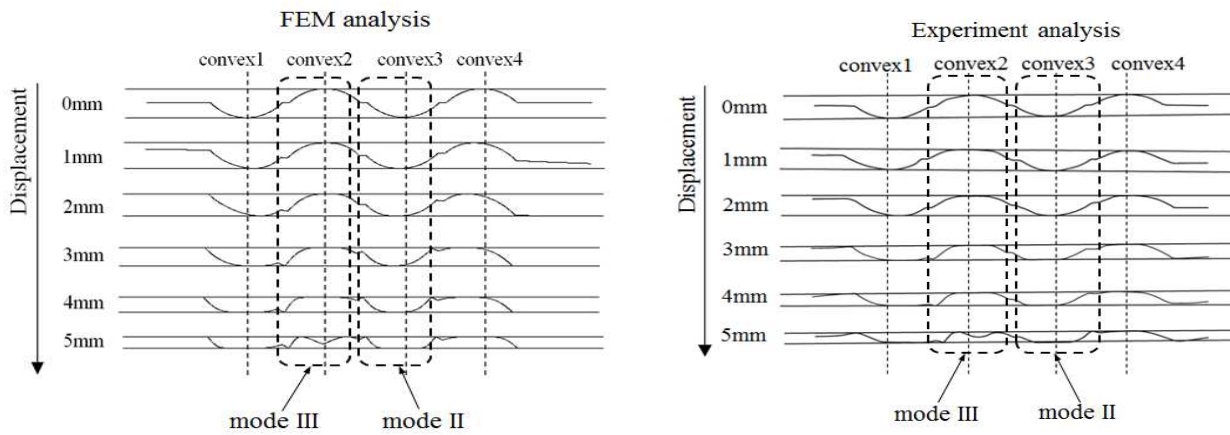


Fig. 6 Deformation mode for gasket having flat portion of 2.0 mm

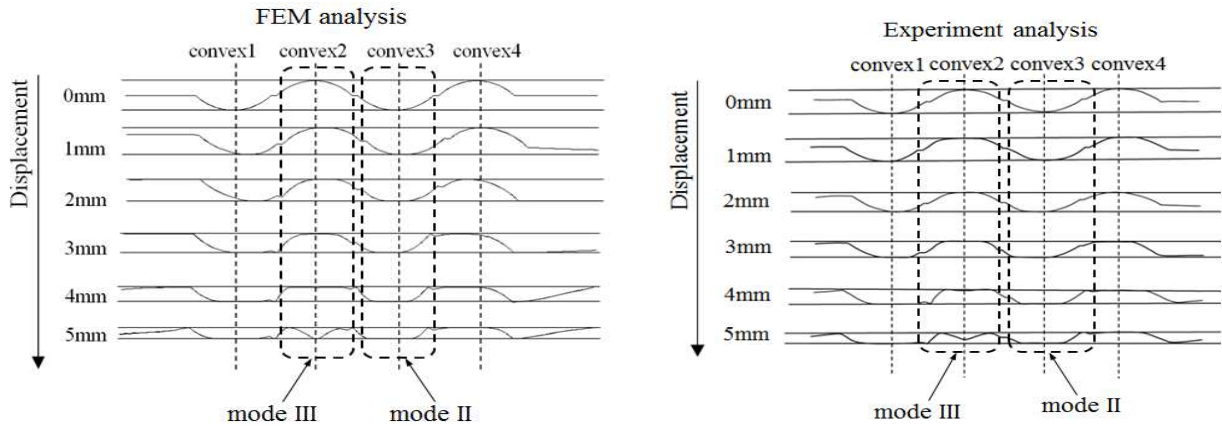


Fig. 7 Deformation mode for gasket having flat portion of 1.5 mm

Fig. 8 shows a distribution map of the deformation modes. The vertical axis is aspect ratio of the length of the flat portion to the length of the convex portion, whereas the horizontal axis is the aspect ratio of the height to the length of the convex portion. Here, the deformation mode of the thin stainless gasket material has a higher probability of deformation in mode I when the aspect ratio of the length of the flat portion to the length of the convex portion, L/D , increases. The deformation maps of the thin stainless gasket material plotted in this study are very important in the design process of the gasket and could function as a key reference in the future.

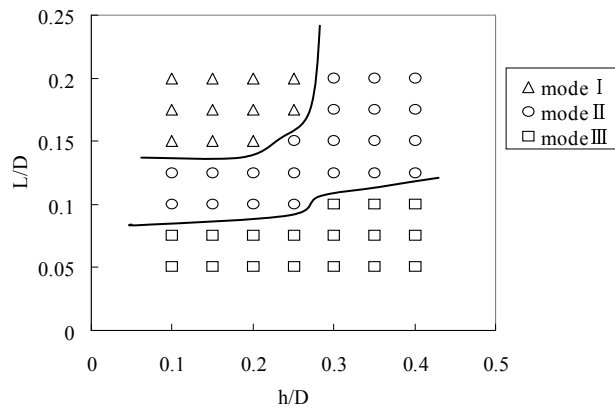


Fig. 8 Deformation map for thin stainless gasket material

Fig. 9 shows the curve correlation between the load and displacement for both the experimental and simulation analysis results. The load increase tended to be constant for a gasket having a flat portion of 4.0 mm with a displacement between 0–4 mm; after this, the load increased significantly. Moreover, for gaskets with flat portions of 1.5 mm and 2.0 mm, the load increased significantly throughout the deformation. A relatively high value for the flat portion produced a decreasing load. There was good correlation between the simulation analysis results and experimental data.

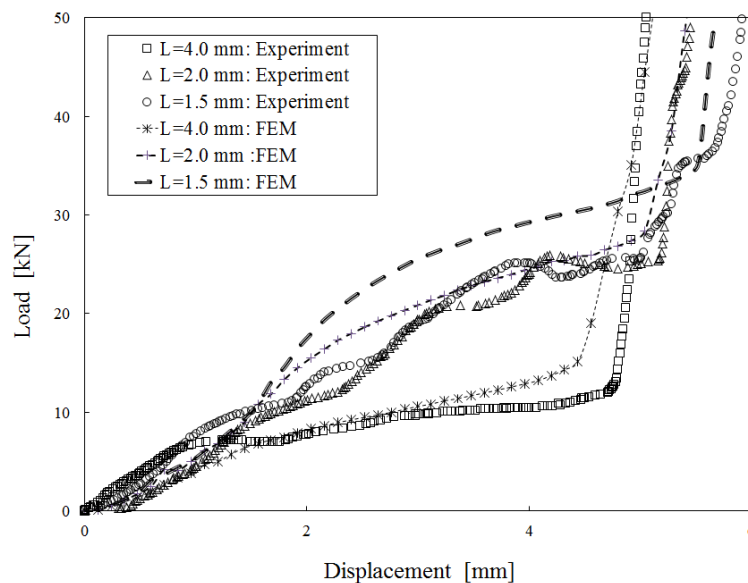


Fig. 9 Load–displacement curve

The simulation analysis obtained the displacement–contact stress and width curves. Fig. 10 shows the relationship between the displacement and contact stress analysis results for flat portions of 4 mm, 2 mm, and 1.5 mm. A gasket having a flat portion of 4.0 mm did not provide a good seal because the contact stress did not increase. In addition, an increase in the displacement increased the contact stress in convex portion 2 (deformation mode III) and convex portion 3 (deformation mode II) for flat portions of 2 mm and 1.5 mm. However, for gaskets with flat portions of 1.5 mm and 2 mm, there was a dent in convex portion 3, shape buckling occurred, and the contact stress decreased rapidly. Therefore, the deformation mode with the best sealing was deformation mode II. Fig. 11 shows the relationship between the displacement and the contact width. In a gasket having a flat portion of 4.0 mm, the contact width in convex portion 2 did not increase when the displacement increased, because the deformation was concentrated in the flat portion. The contact width in portion 2 for a gasket having a flat portion of 2.0 mm and the contact width in portion 3 for a gasket having a flat portion of 1.5 mm increased significantly when the displacement increase started from 3 mm.

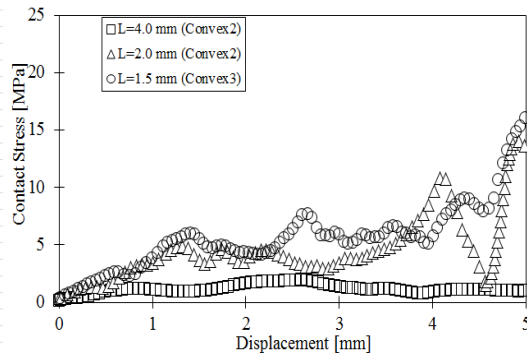


Fig. 10 Displacement-contact stress curve

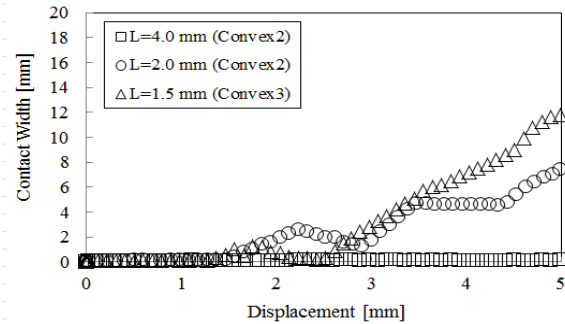


Fig. 11 Displacement-contact width curve

Conclusions

In this research, based on simulation and experimental analyses, we can conclude that:

- 1) By comparing the analytical and experimental results, although some errors occurred, the validity of the finite element model was clarified.
- 2) Based on the FEM analysis results, the mode analysis could be divided into three types of deformation modes. In deformation mode I, the convex portion was undeformed whereas the flat portion was deformed. In deformation mode II, the convex portion was deformed whereas the flat portion remained undeformed. Deformation mode III was the same as deformation mode II, but dent geometrical buckling occurred. Therefore, deformation mode II provided the best sealing.
- 3) Increasing the length of the flat portion decreased the load and caused deformation mode II to change to deformation mode III and then deformation mode I.
- 4) In deformation mode III, although it was possible to obtain both a high contact stress and high contact width, the contact stress rapidly decreased because there was a recessed protrusion.

Acknowledgements

This project was supported by the Strength of Material Laboratory, Yamaguchi University, Japan. The second author is grateful for the scholarship support from the Directorate of Higher Education Indonesia in cooperation with Yogyakarta State University.

References

- [1] Saeed, H.A, Izumi, S., Sakai, S., Haruyama, S., Nagawa, M., Noda, H., Development of New Metallic Gasket and its Optimum Design for Leakage Performance, *Journal of Solid Mechanics and Material Engineering*, Vol. 2, No. 1 (2008), 105–114.
- [2] Haruyama, S., Choiron, M.A., Kaminishi, K., A Study of Design Standard and Performance Evaluation on New Metallic Gasket, *Proceeding of the 2nd International Symposium on Digital Manufacturing, Wuhan China*, (2009), 107–113.
- [3] Choiron, M.A., Haruyama, S., Kaminishi, K., Simulation and Experimentation on the Contact Width of New Metal Gasket for Asbestos Substitution, *International Journal of Aerospace and Mechanical Engineering*, Vol. 5, No. 4 (2011), 283–287.
- [4] Nurhadiyanto, D., Choiron, M.A., Haruyama, S., Kaminishi, K., Optimization of New 25A-size Metal Gasket Design Based on Contact Width Considering Forming and Contact Stress Effect, *International Journal of Mechanical and Aerospace Engineering*, Vol. 6 (2012), 343-347.
- [5] Ushijima, K., Haruyama, S., Kaminishi, K., Study on Deformed Mode of Metal Seal Materials Using Elastic Effect, *Proceeding of the 8th International Conference on Innovation and Management*, (2011).
- [6] JIS Z2241, *Metallic materials-Tensile testing-Method of test at room Temperature*, Japanese Standards Association, (2011).